Protein methionine oxidation mediates reperfusion injury in acute ischemic stroke

Sean X. Gu, Ilya O. Blokhin, Katina M. Wilson, Nirav Dhanesha, Prakash Doddapattar,

Isabella M. Grumbach, Anil K. Chauhan, and Steven R. Lentz

Supplemental Figures

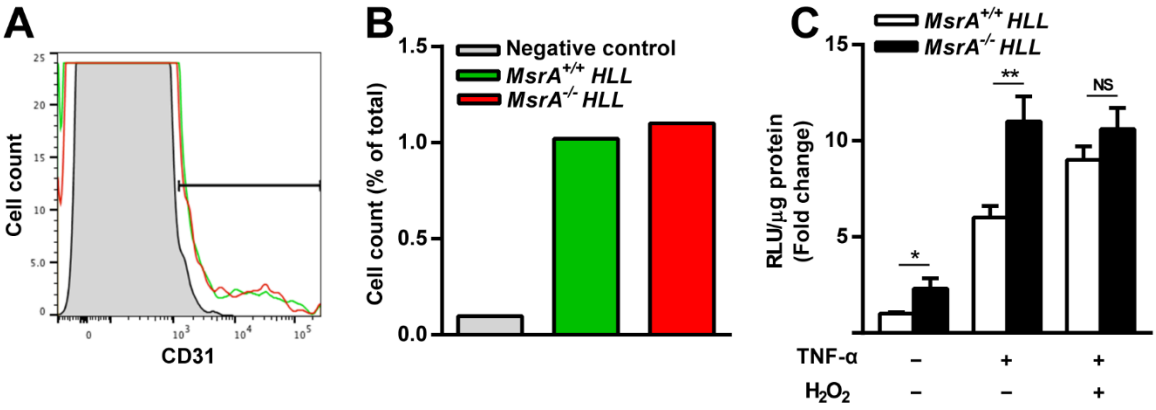

Figure S1. NF-κB activation is regulated by methionine oxidation in isolated brain microvascular endothelial cells (BMVEC). (A) Fluorescence-activated cell sorting of CD31-positive single-cell suspensions prepared from brain tissue of *MsrA+/+ HLL* (red) or *MsrA-/- HLL* (green) mice. Unstained negative control (shaded area) was used to determine the gating parameters for sorting. **(B)** Graphical representation of the number of isolated CD-31 positive cells as a percentage of total cells. Brains from three mice in each group were pooled to maximize yield. **(C)** Isolated brain microvascular endothelial cells from *MsrA*$^{+/+}$ *HLL* or *MsrA*$^{-/-}$ *HLL* mice were treated with TNF-α (2 ng/ml) and H_2O_2 (30 µM) as indicated. After 4 hours, cell lysates were isolated and assayed for NF-κB activity by a luciferase enzymatic assay. Results are expressed as mean RLU ± SEM after normalization for total protein and for luciferase activity in PBS treated controls (n = 4). **(B)** Two sided, unpaired Student's *t* test. **(C)** Two-way ANOVA with Sidak's multiple comparisons test. **P* < 0.05; ***P* < 0.01

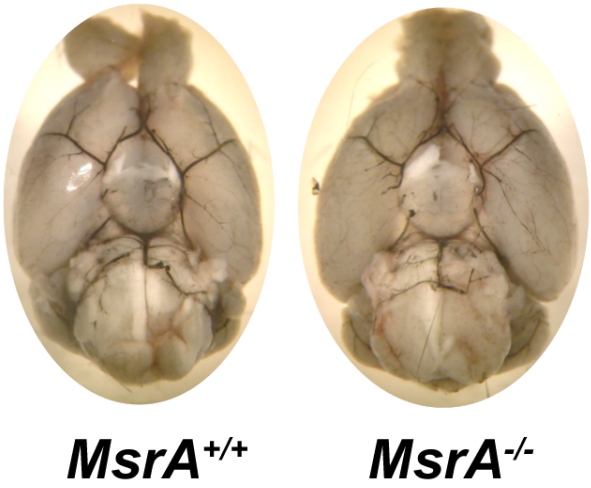

Figure S2. Comparison of cerebrovascular anatomy between *MsrA*$^{+/+}$ and *MsrA*$^{-/-}$ mice. Inferior view of the brain from mice given an intracardiac injection of India ink. Circle of Willis and major communicating arteries (black) were comparable between *MsrA*$^{+/+}$ and *MsrA*$^{-/-}$ mice indicating no strain-related differences in gross cerebrovascular anatomy.

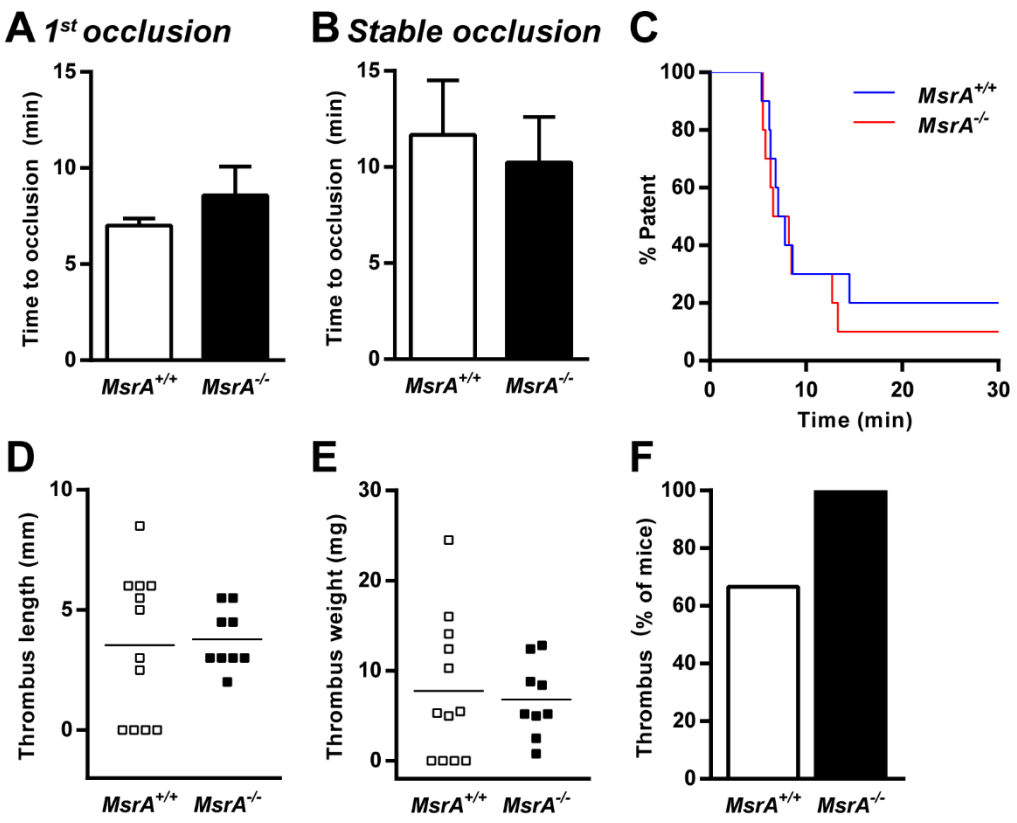

Figure S3. Susceptibility of *MsrA*$^{+/+}$ and *MsrA*$^{-/-}$ mice to experimental thrombosis. **(A-C)** Experimental arterial thrombosis using $FeCl_3$ model of carotid artery injury. **(A)** Time to first occlusion, **(B)** time to stable occlusion, and **(C)** percent patency of carotid artery after injury (n = 10-11). **(D-F)** Experimental venous thrombosis using inferior venal cava ligation model. **(D)** Thrombus length, **(E)** thrombus weight, and **(F)** percentage of mice developing thrombus after ligation of the inferior vena cava (n = 9-12). **(A, B)** Mann-Whitney *U* test. **(C)** Log rank test. **(D-F)** Two-sided, unpaired Student's *t* test.

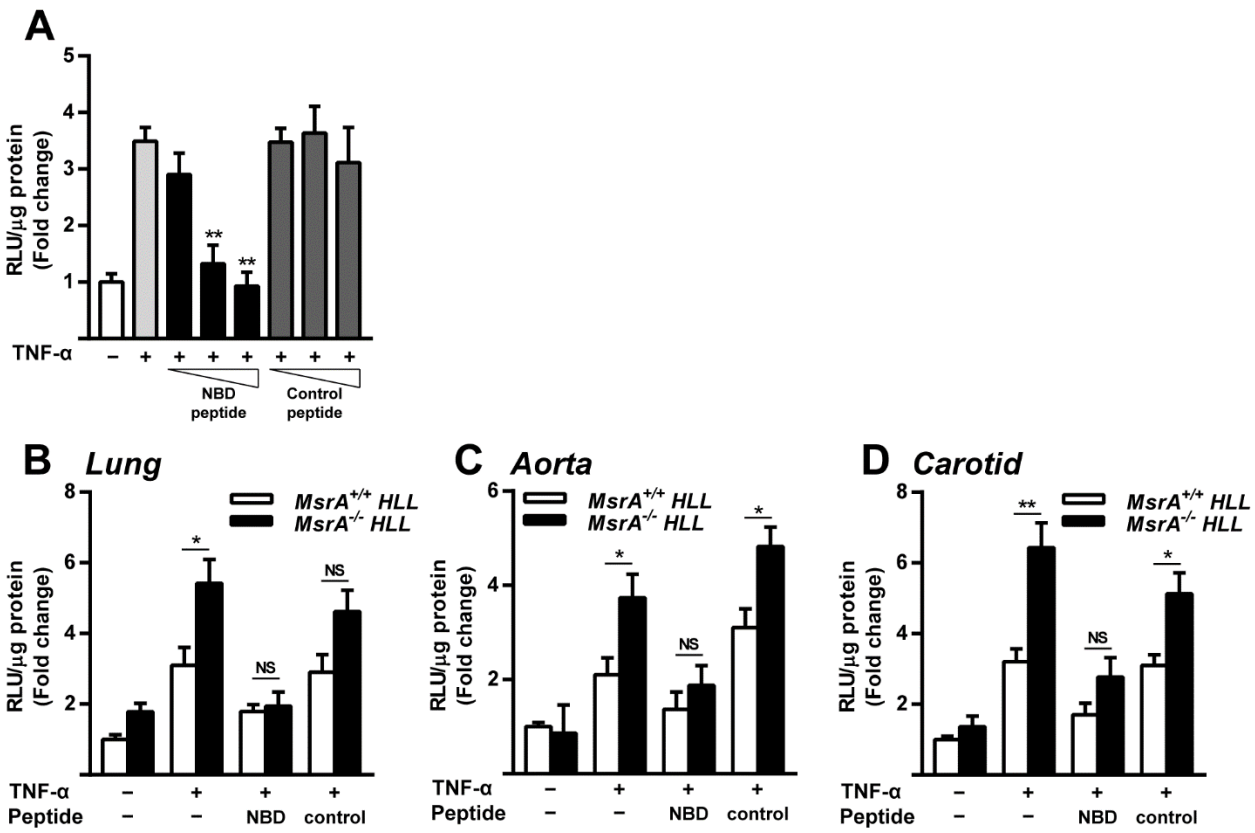

Figure S4. NF-κB inhibition by NBD peptide *in vitro* and *in vivo*. (A) HUVECs were cultured and infected with an adenoviral NF-κB reporter, Ad-NF-κB-Luc. At 40 hours post-infection, cells were stimulated with 2 ng/ml of TNF-α along with increasing concentrations (2, 20, or 200 μM) of NBD peptide or control peptide. After 4 hours, NF-κB activity was assessed by a luciferase enzymatic assay. Results are normalized for total protein and for luciferase activity in untreated cells. Data are expressed as mean RLU ± SEM (n = 4). **P* < 0.05 vs. TNF-α stimulated control. **(B)** NF-κB activity was assessed by luciferase enzymatic assay in the lung, aorta, and carotid arteries of *MsrA*$^{-/-}$ *HLL* or *MsrA*$^{+/+}$ *HLL* mice after 4 hours treatment with TNF-α (1 mg/kg IP) or vehicle control (PBS) along with either NBD (2 mg/kg IP) or control peptide. Results were normalized for total protein and for luciferase activity in wild-type controls. Data are expressed as mean RLU ± SEM (n = 4-6 for each group). **(A)** One-way ANOVA with Tukey's multiple comparisons test. **(B-D)** One-way ANOVA with Tukey's multiple comparisons test. **P* < 0.05; ***P* < 0.01